

An Experimental Technique for the Generation of Large-Scale Spanwise Vortices in a Wind Tunnel

M.J. Emes, F. Ghanadi, M. Arjomandi and R.M. Kelso

Department of Mechanical Engineering
University of Adelaide, Adelaide, South Australia 5005, Australia

Abstract

The presence of large-scale vortices with high spanwise coherence has been observed in the atmospheric boundary layer (ABL). This study investigates an innovative technique to generate a large-scale spanwise vortex from the oscillation of a surface-mounted fence in a wind tunnel. Characteristics of the large vortex with a well-defined length scale and its development with downstream distance behind the fence were investigated. Time-averaged profiles of velocity, normal and Reynolds stresses were measured to determine the dominant frequencies of the large vortices in the wake of the oscillating fence. Longitudinal length scales of the spanwise vortices were calculated using the autocorrelation of velocity data. It was found that the size of the largest spanwise vortices are most significantly influenced by the height of the fence, such that the integral length scales increased by 52mm for a 20mm increase in fence height. Spanwise vortices were also found to be 11mm larger when oscillating the fence at the vortex shedding frequency behind a stationary fence. The oscillation amplitude of the fence was found to have a negligible effect on the size of the large spanwise vortices.

Introduction

Characterisation of coherent structures in the lower atmospheric boundary layer (ABL) requires an understanding of turbulent phenomena that are responsible for gusts on small physical structures such as heliostats and dynamic wind loads on large civil structures. Wind codes and standards adopt a quasi-steady gust factor approach based on a maximum gust wind speed and turbulence intensity for the estimation of peak wind loads, however the dynamic response of large civil structures is more significantly influenced by the frequency distribution of the longitudinal velocity and the size of the largest eddies in the ABL [5]. There exists a wide range of turbulent structures within the ABL, such as very large superstructures observed as counter-rotating pairs of horseshoe vortices in the logarithmic region [6, 11]. Spanwise vortices with an axis of rotation perpendicular to the flow are components of these superstructures resulting from the interaction of separating and reattaching shear layers and tripping around obstacles on the ground [17]. The presence of large-scale eddies with high spanwise coherence has been observed in the shear layer, even for significant levels of free-stream turbulence from small-scale buffeting [20]. Coherent structures within canonical turbulent boundary layers have typically been quantified through the measurement of planar vortices such as spanwise vortices, however these structures are yet to be fully quantified from high resolution velocity measurements in the ABL because of the limited number of vertical data points along the height of a wind mast [16].

Large-scale spanwise vortices have been found to be responsible for most of the entrainment in the naturally occurring shear layer, leading to dynamic responses of large structures such as buildings and bridges. Large eddies of a similar size to the

structure result in well correlated pressures over its surface as the eddy engulfs the structure, leading to maximum wind loads [4, 12]. Structural failure due to excessive deflections and stresses from galloping and torsional flutter tend to occur at small frequencies of the order of 1 Hz when the turbulence length scales are comparable to the size of the body, however the effect becomes negligible when turbulence scale is increased beyond the order of magnitude of the body scale [13]. The size of the largest eddies is defined by the integral length scale in the inertial subrange of frequencies in the ABL [7]. The longitudinal integral length scale xL_u (m) at a given height is defined as the streamwise spacing between two-dimensional spanwise vortices orientated in the axial direction. Hence, the aim of this paper is to characterise the size of a large spanwise vortex that physical structures are likely to be exposed to in the ABL.

Time-averaged and phase-averaged measurements of velocity characteristics have previously been used to identify, analyse and characterise large-scale vortex structures within the separated shear layer in turbulent flows such as behind bluff bodies [15]. The near wake behind bluff bodies is affected by flow separation and reattachment and vortex shedding, with the associated length scales of the shear layer thickness and the spacing between the two separated shear layers given by the body height respectively [13]. Periodic motions in the form of a von Karman vortex street behind circular cylinders and flat plates have been widely studied in the literature through flow visualisation, conditional averaging techniques and spectral analyses. A body is defined as bluff if there is separated flow over a substantial proportion of its surface, however the isolation of a single coherent large-scale vortex in the wake of bluff bodies has proven to be difficult at high Reynolds numbers above 20,000 because of the development of instabilities and the interaction of unsteady vortices [1]. The generation of large two-dimensional spanwise vortices has been most effectively produced by the forcing of periodic motions in the shear layer [8]. This has previously been investigated using several dynamic methods, such as oscillating cylinders and airfoils to generate large spanwise vortex structures. However, the limitation of cylindrical bluff bodies with a change of surface curvature is that shed vortices exhibit larger spanwise waviness and dispersion in streamwise spacing [10]. Alternatively, there is a straight line of flow separation from a rectangular plate that is fixed at its edges, leading to more coherent vortices with well-defined length scales. Small-amplitude sinusoidal oscillations of a floor-mounted normal plate in the streamwise direction have previously been demonstrated by Kelso *et al.* [9] to generate large-scale spanwise vortices with improved coherence and periodicity compared to a stationary fence. Hence, the scope of this study is to investigate the effect of oscillation amplitude, oscillation frequency and height of a floor-mounted normal flat plate on the integral length scales of the largest vortices behind the oscillating fence.

Experimental Setup

Oscillating Fence in Boundary Layer Rig

Experimental measurements were taken in a closed return wind tunnel at the University of Adelaide. Figure 1 shows the schematic layout of the boundary layer rig containing an acrylic flat plate with an elliptical leading edge for minimal flow separation from the plate and smooth development of the boundary layer. The flat plate has previously been designed with a $0.5 \text{ m} \times 0.3 \text{ m}$ cross-section and 2.15 m test section length. Plexiglass side walls of the test section are adjustable to control pressure gradient along the flat plate. An adjustable angle trailing edge flap of 0.2 m length is also used to ensure the stagnation point is on the measurement side of the plate and the boundary layer is developed smoothly. The upstream boundary layer was perturbed using a 3 mm trip wire, giving a boundary layer thickness δ of 25 mm ($\delta/h = 0.31$) at the position of the fence. The free-stream turbulence intensity at the tunnel's centreline was measured at 0.5%.

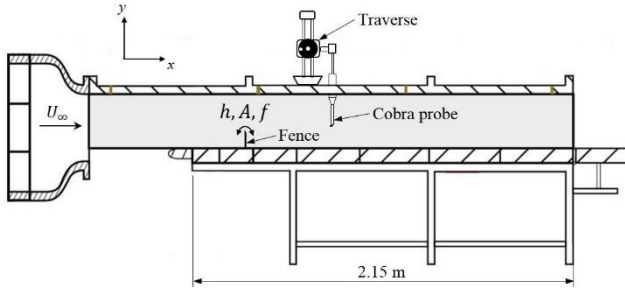


Figure 1. Schematic diagram of the traversing mechanism and the boundary layer rig in the wind tunnel.

A thin rectangular plate of 60mm height (h) with aspect ratio (w/h) of 4.17 was mounted spanwise to the surface of the acrylic plate using hinges in the boundary layer rig, as shown in Figure 2. One end of the aluminium fence was connected to a high-torque JR ES579 servo motor via a horn pin, as shown inset in Figure 2. The servo motor was controlled by an Arduino Uno microcontroller through Matlab to oscillate the fence at frequencies from 1-10 Hz and amplitudes between 2mm and 12mm. Velocities were measured in the wake using a high-frequency Cobra probe for over 25 oscillation cycles of the fence. The free-stream Reynolds number Re_∞ was approximately 28,000 based on the fence height and the freestream velocity $U_\infty = 7 \text{ m/s}$. The Reynolds number Re_x based on the distance x behind the fence was in the range between 100,000 and 280,000. The top edge of the fence was chamfered at 30° to ensure clean separation and controlled generation of spanwise vortices was achieved by oscillating the fence at a peak-to-peak amplitude A of 4mm ($A/h = 0.03$) and forcing frequency $f = 5 \text{ Hz}$ corresponding to a Strouhal number of 0.043 and fence-tip velocity of approximately 0.04 m/s.

Flow Measurement Technique

A Turbulent Flow Instrumentation (TFI) Cobra pressure probe was used to measure the flow in the wake of the oscillating fence. The multi-hole probe with 2.5 kPa pressure transducers was dynamically calibrated by the manufacturer to allow accurate flow measurements up to 90 m/s and provide a frequency response up to 2 kHz as a more robust alternative to hot-wire anemometers. The probes were able to resolve the three orthogonal components of velocity and static pressure, as long as the flow vector was contained within a cone of $\pm 45^\circ$ around the probe x -axis [19]. This enabled resolution of the constantly fluctuating velocity vector in the turbulent flow when the probe

was approximately aligned with the freestream flow direction and the turbulence intensities were not excessively large ($I_u < 30\%$).

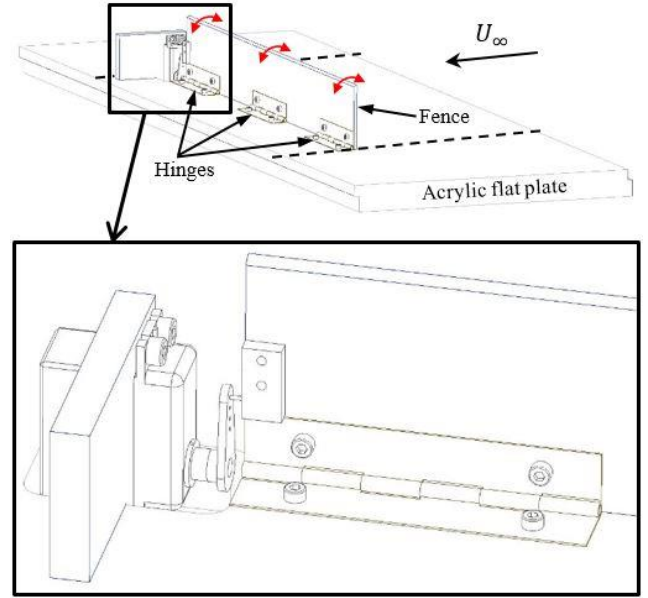


Figure 2. Schematic diagram showing the oscillating fence hinged to the acrylic flat plate. Dashed lines indicate the location of the Plexiglass side walls of the boundary layer rig. The inset shows the connection of the servo motor to the fence via a servo horn pin.

Integral Length Scales

The sizes of the largest eddies in the wake of the oscillating fence are defined by the integral length scale xL_u at the lower bound of the inertial subrange frequency domain in the ABL [7]. Point velocity measurements as a function of time are transformed to spatially distributed data by adopting Taylor's hypothesis that eddies are embedded in a frozen turbulence field, which is convected downstream at the mean wind speed \bar{U} (m/s) in the streamwise x -direction and hence do not evolve with time [7]. The integral length scale at a given height in the ABL is therefore calculated as [14, 18]

$$^xL_u = ^xT_u \bar{U}, \quad (1)$$

where xT_u (s) is the integral time scale representing the time taken for the largest eddies to traverse the inertial subrange in the ABL before they are dissipated by viscosity at the Kolmogorov length scale η . Integral time scales are commonly estimated from the covariance of single point velocity data between two different times using the normalised autocorrelation function $R_u(\tau)$ of the fluctuating turbulent component of the velocity [7]

$$R_u(\tau) = \frac{\overline{u'(t)u'(t+\tau)}}{\overline{u'(t)u'(t)}} \quad (2)$$

Here τ (s) is the time lag with respect to time t over which $R(\tau)$ decreases in magnitude from one to zero as $u'(t + \tau)$ becomes uncorrelated and statistically independent of $u'(t)$. The autocorrelation function is calculated from the velocity data using the `xcorr` function in Matlab. The integral time scale is defined by

$$^xT_u = \int_0^\infty R_u(\tau) d\tau \approx \int_0^{\tau_0} R_u(\tau) d\tau, \quad (3)$$

where the integral is taken to the first-zero crossing τ_0 of the autocorrelation function by assuming that $R(\tau)$ fluctuates very close to zero after this point [14, 18]. Alternatively xT_u is

approximated from the frequency at the peak of the Engineering Sciences Data Unit [2] power spectral density (PSD) function derived from the von Karman spectral equations and fitted to the measured data [3].

Results

Time-Averaged Velocity and Stress Profiles

Figure 4 presents the time-averaged u and v velocity profiles in the streamwise x and vertical y directions, which have been non-dimensionalised with respect to the freestream velocity U_∞ . Mean u -velocity profiles in Figure 4(a) at the two closest positions behind the fence are negative for $y/h \leq 1$, which shows that there is recirculation in the near-wake region directly behind the fence as the shear layer has detached from the wall surface around the oscillating fence. The mean streamwise velocity u at the closest measurement height to the ground ($y/h = 0.1$) is approximately zero at $x/h = 8$, which indicates that the reattachment length is approximately $8h$ for the oscillating fence, compared to $10h$ for the stationary fence. It is also apparent from Figure 4(a) that measurements did not extend to the height of the shear layer where $\bar{u}/U_\infty = 1$ at all streamwise positions. Mean vertical v -velocity profiles in Figure 3(b) are close to zero and show some scatter in the recirculation region, however they become negative with increasing height as the shear layer reattaches downstream.

The time-averaged profiles of Reynolds stresses as a function of the streamwise position behind the fence have also been investigated. As shown in Figure 4(a), the peak stresses occur at the middle of the shear layer around $y/h = 1.5$ at the two nearest positions behind the fence and show a general decrease in magnitude with streamwise distance. The maximum Reynolds shear stress occurs at $x/h = 5$, which is an indication of turbulent stress production and rapid shear layer growth from the direct roll-up of large-scale eddies. The stress profiles at $x/h = 8$ and 10 in Figure 4(b) show that the shear stresses are comparable to those measured by Kelso *et al.* [9], however the maximum Reynolds stresses are 13% lower due to the smaller forcing velocity of the fence relative to the freestream velocity in this study.

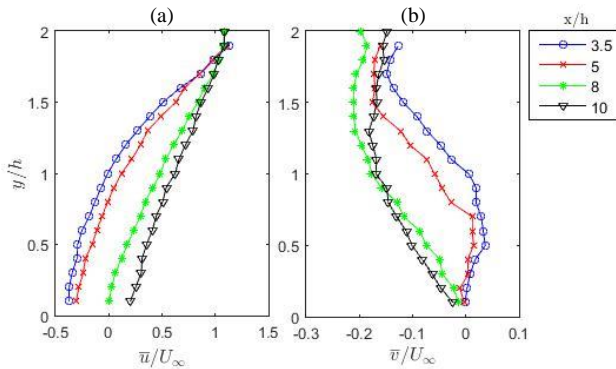


Figure 3. Time-averaged velocity profiles: (a) Streamwise, (b) Vertical; normalised to the freestream velocity U_∞ at four downstream distances of the 60mm oscillating fence ($A/h = 0.03$, $f = 5$ Hz).

(a) (b)

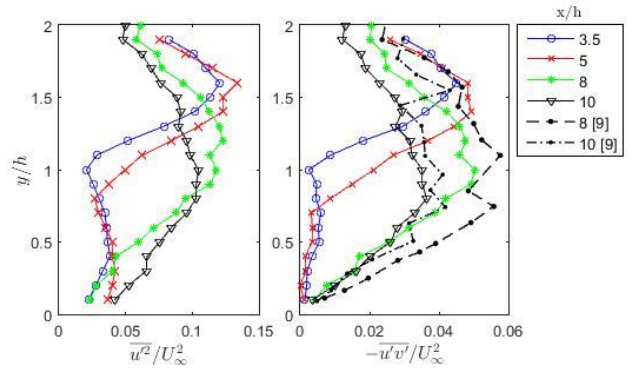


Figure 4. (a) Streamwise normal stress $\overline{u^2}/U_\infty^2$; (b) Reynolds shear stress $-\overline{u'v'}/U_\infty^2$ compared with experimental data [9].

Integral Length Scales

Figure 5(a) shows that the length scales of eddies are the order of the fence height, increasing with height in the reattaching shear layer to $1.27h$ and $1.37h$ respectively at $x/h = 8$ and 10 respectively. The maximum gradient in the shear layer occurs further upstream at $x/h = 3.5$, where the spanwise vortices roll up and merge as the separated shear layer develops downstream. Hence, the largest eddies are expected to be developed into a well-organised shape in the region around reattachment at $x/h \geq 8$. With further distance downstream at $x/h \geq 12$, the vortices become elongated and hence the longitudinal integral length scale xL_u increases to a maximum value of $2h$.

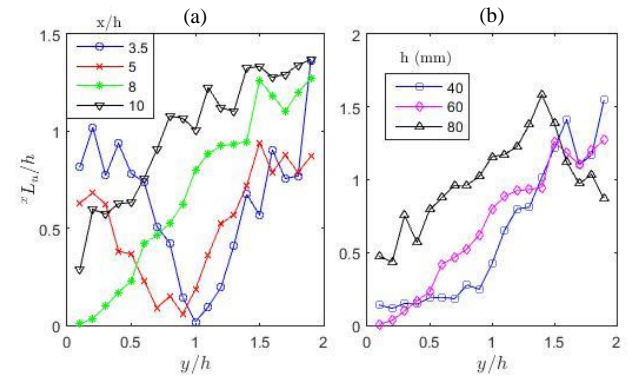


Figure 5. (a) Integral length scale profiles calculated using the autocorrelation function as a function of downstream distance (x/h) and non-dimensionalised with the height of the oscillating fence ($h = 60$ mm); (b) Effect of fence height on integral length scales at $x/h = 8$ downstream of the oscillating fence ($A/h = 0.03$, $f = 5$ Hz).

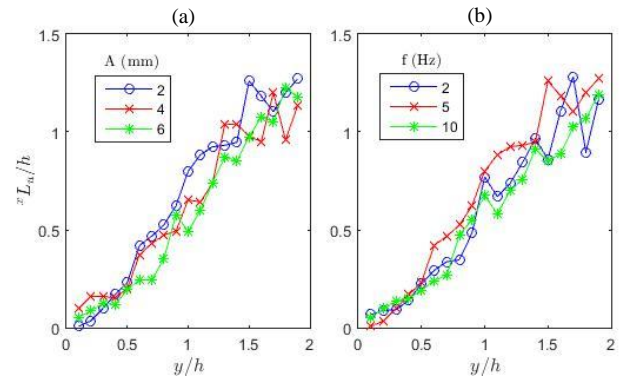


Figure 6. Effect of oscillation (a) amplitude A , and (b) frequency f on integral length scales at $x/h = 8$ downstream of the 60mm fence.

Figure 5(b) shows that the size of the largest spanwise vortices at $x/h = 8$ and the largest gradients of increasing xL_u occur at heights around the middle of the reattaching shear layer

($0.5 < y/h < 1.5$). The integral length scale non-dimensionalised by the fence height $^xL_u/h$ increases with height to a peak value shown in Table 1, before decreasing and fluctuating after this point. The position of the largest spanwise vortices become closer to the wall with increasing fence height at $x/h = 8$. This is believed to be due to increased blockage of the tunnel with increasing fence height.

h (mm)	$^xL_u/h$	y/h
40	1.41	1.6
60	1.26	1.5
80	1.59	1.4

Table 1. Sizes of the largest spanwise vortices and their position within the shear layer at $x/h = 8$ as a function of fence height.

Figure 6(a) shows that the integral length scale profiles at $x/h = 8$ are not significantly influenced by a change in the amplitude of the sinusoidal oscillation of the 60mm fence. However, the largest spanwise vortices are generated at an oscillation frequency of 5 Hz in Figure 6(b), which is close to the vortex shedding frequency for a stationary fence. Forcing the shear layer at this frequency appears to cause the direct roll-up of large-scale two-dimensional vortices [9], Hence, a 5 Hz oscillation frequency was used as the operating point in this study.

Discussion

It is clear that the forcing of the fence leads to substantial change in the development of the shear layer, leading to more rapid shear layer growth and turbulent stress production. The maximum Reynolds shear stresses show that the development of large-scale vortices through merging and direct roll-up mechanisms at $x/h = 5-8$ corresponds to the vortices with the largest integral length scales. The largest vortices continue to increase in size after shear layer reattachment at $x/h = 8$ as they become elliptical due to vortex stretching.

The results show that the largest spanwise vortices are most significantly affected by changes in the fence height. The maximum integral length scale increases by 52mm (26%) in the middle of the shear layer when the fence height increases from 60mm to 80mm. In comparison, the length scales in the middle of the shear layer ($0.5 < y/h < 1.5$) are 11mm (18%) larger for a 5 Hz oscillation frequency than for 2 Hz and 10 Hz. This suggests that this frequency of oscillation has enhanced the roll-up mechanism of vortices from the tip of the fence that have developed to become larger further downstream.

There are some experimental errors in the calculation of integral length scales. Time samples of the order of 10 minutes to 1 hour would usually be required in the ABL, however only 5 second time samples were possible in this study due to the large quantity of measurements required. Taylor's hypothesis of frozen turbulence implies the assumption that the constant mean velocity is large with respect to the turbulence fluctuations and combined with the 2 m/s lower measurement limit of the Cobra probe, the integral length calculated for $y/h < 0.7$ at $x/h = 8$ are considered to be a rough estimate with a larger error. The limitation of the probe's cone of acceptance also leads to uncertainty of the length scales in the recirculation region at $x/h = 3.5$ and 5. However, after reattachment at $x/h = 8$ and 10 the integral length scales calculated using the first-zero crossing method are estimated to have a 95% confidence interval assuming a Gaussian distribution.

Conclusion

Wind tunnel results have shown that large spanwise vortices are generated by the forcing of the shear layer behind an oscillating

fence. The integral length scales of these vortices are significantly affected by the fence height, such as a 26% increase in the maximum length scale when increasing the fence height from 60mm to 80mm. The amplitude of the fence oscillation has a negligible influence on the size of the largest vortices at the downstream position of shear layer reattachment. However, the average integral length scale of vortices in the middle region of the shear layer can be increased by 18% when the frequency of oscillation is approximately equal to the vortex shedding frequency for a stationary fence.

Acknowledgments

This work has been supported by the Australian Solar Thermal Research Initiative (ASTRI), through funding provided by the Australian Renewable Energy Agency (ARENA).

References

- [1] Bearman, P.W., Vortex shedding from oscillating bluff bodies, *Annual review of fluid mechanics*, **16**, 1984, 195-222.
- [2] Engineering Sciences Data Unit, ESDU 85020: Characteristics of Atmospheric Turbulence Near the Ground. Part II: Single Point Data for Strong Winds, 2001.
- [3] Flay, R.G.J. & Stevenson, D.C., Integral length scales in strong winds below 20 m, *Journal of Wind Engineering and Industrial Aerodynamics*, **28**, 1988, 21-30.
- [4] Greenway, M.E., An analytical approach to wind velocity gust factors, *Journal of Wind Engineering and Industrial Aerodynamics*, **5**, 1979, 61-91.
- [5] Holdø, A.E., Houghton, E.L. & Bhinder, F.S., Some effects due to variations in turbulence integral length scales on the pressure distribution on wind-tunnel models of low-rise buildings, *Journal of Wind Engineering and Industrial Aerodynamics*, **10**, 1982, 103-115.
- [6] Hutchins, N. & Marusic, I., Evidence of very long meandering features in the logarithmic region of turbulent boundary layers, *Journal of Fluid Mechanics*, **579**, 2007, 1-28.
- [7] Kaimal, J.C. & Finnigan, J.J., *Atmospheric Boundary Layer Flows: Their Structure and Measurement*, Oxford University Press, 1994.
- [8] Kelso, R.M., A Study of Free Shear Flows Near Rigid Boundaries, Thesis: Doctor of Philosophy in Mechanical Engineering, University of Melbourne, 1991.
- [9] Kelso, R.M., Lim, T.T. & Perry, A.E., The effect of forcing on the time-averaged structure of the flow past a surface-mounted bluff plate, *Journal of Wind Engineering and Industrial Aerodynamics*, **49**, 1993, 217-226.
- [10] Kiya, M. & Matsumura, M., Incoherent turbulence structure in the near wake of a normal plate, *Journal of Fluid Mechanics*, **190**, 1988, 343-356.
- [11] Marusic, I. & Hutchins, N., Study of the log-layer structure in wall turbulence over a very large range of Reynolds number, *Flow, Turbulence and Combustion*, **81**, 2008, 115-130.
- [12] Mendis, P., Ngo, T., Haritos, N., Hira, A., Samali, B. & Cheung, J., Wind loading on tall buildings, *EJSE Special Issue: Loading on Structures*, **3**, 2007, 41-54.
- [13] Nakamura, Y., Bluff-body aerodynamics and turbulence, *Journal of Wind Engineering and Industrial Aerodynamics*, **49**, 1993, 65-78.
- [14] O'Neill, P.L., Nicolaidis, D., Honnery, D. & Soria, J., Autocorrelation functions and the determination of integral length with reference to experimental and numerical data, in *15th Australasian Fluid Mechanics Conference*, 2004, 13-17.
- [15] Perry, A.E. & Steiner, T.R., Large-scale vortex structures in turbulent wakes behind bluff bodies. Part 1. Vortex formation processes, *Journal of fluid mechanics*, **174**, 1987, 233-270.
- [16] Rosi, G.A., Martinuzzi, R.J. & Rival, D.E., A conditional analysis of spanwise vortices within the lower atmospheric log

layer, *Journal of Wind Engineering and Industrial Aerodynamics*, **119**, 2013, 89-101.

[17] Sarkar, P.P., Techniques and tools for assessing extreme-wind hazard to structures, in *8th Asia-Pacific Conference on Wind Engineering*, 2013, 131-172.

[18] Swamy, N.V.C., Gowda, B.H.L. & Lakshminath, V.R., Auto-correlation measurements and integral time scales in three-dimensional turbulent boundary layers, *Applied Scientific Research*, **35**, 1979, 237-249.

[19] Watkins, S., Turbulence Characteristics of the Atmospheric Boundary Layer and Possibilities of Replication for Aircraft, in *Joint Symposium of DFG and DLR-Airbus "Third-Symposium-Simulation of Wing and Nacelle Stall"*, 2012, 21-22.

[20] Wygnanski, I., Oster, D., Fiedler, H. & Dziomba, B., On the perseverance of a quasi-two-dimensional eddy-structure in a turbulent mixing layer, *Journal of Fluid Mechanics*, **93**, 1979, 325-335.